CHAPTER 4
DISCUSSION

The structural evolution and the stratigraphy can be interpreted from seismic reflections of the Pattani Basin as demonstrated by Pradidtan and Dook (1992); Lian and Bradley (1986); Chinbunchorn et al. (1989); Crossley (1990) and Lockhart et al. (1997).

The study area consists mainly of N-S to NNW-SSE trending fault sets. Packham (1993) and Polachan et al. (1989) described that the Tertiary basins in the Gulf of Thailand are north-south trending grabens and half-grabens. This N-S trend suggests E-W extension.

4.1 Stratigraphy

The stratigraphy of the study area was described based on seismic interpretation (Crossley, 1990). The variety of depositional environments in the Pattani basin is related to major structures and the direction of sediment source. Six horizons interpreted in this study are compared to stratigraphic units of Crossley (1990) (Figure 4.1). The age of sediment in the study area is Lower Miocene to Upper Miocene. Unit 1 is in sequence 2 - interbedded grey shales / red beds, fluvial point bar, channel sand and locally overpressured coal. Unit 2 overlaps sequences 2 and 3 - grey shales and coals. Unit 3 overlaps sequences 3 and 4 - red beds, point bars, channel sands and few coals. Unit 4 overlaps sequences 4 and 5 - grey claystones, extensive coals and shales, point bars and channel sands. Unit 5 correlates to sequence 5.

The reflectors below horizon D was tilted to the east but those above the horizon are horizontal. These suggest an unconformity between Units 3 and 4 that correlates to the Mid-Miocene Unconformity (Crossey, 1990).

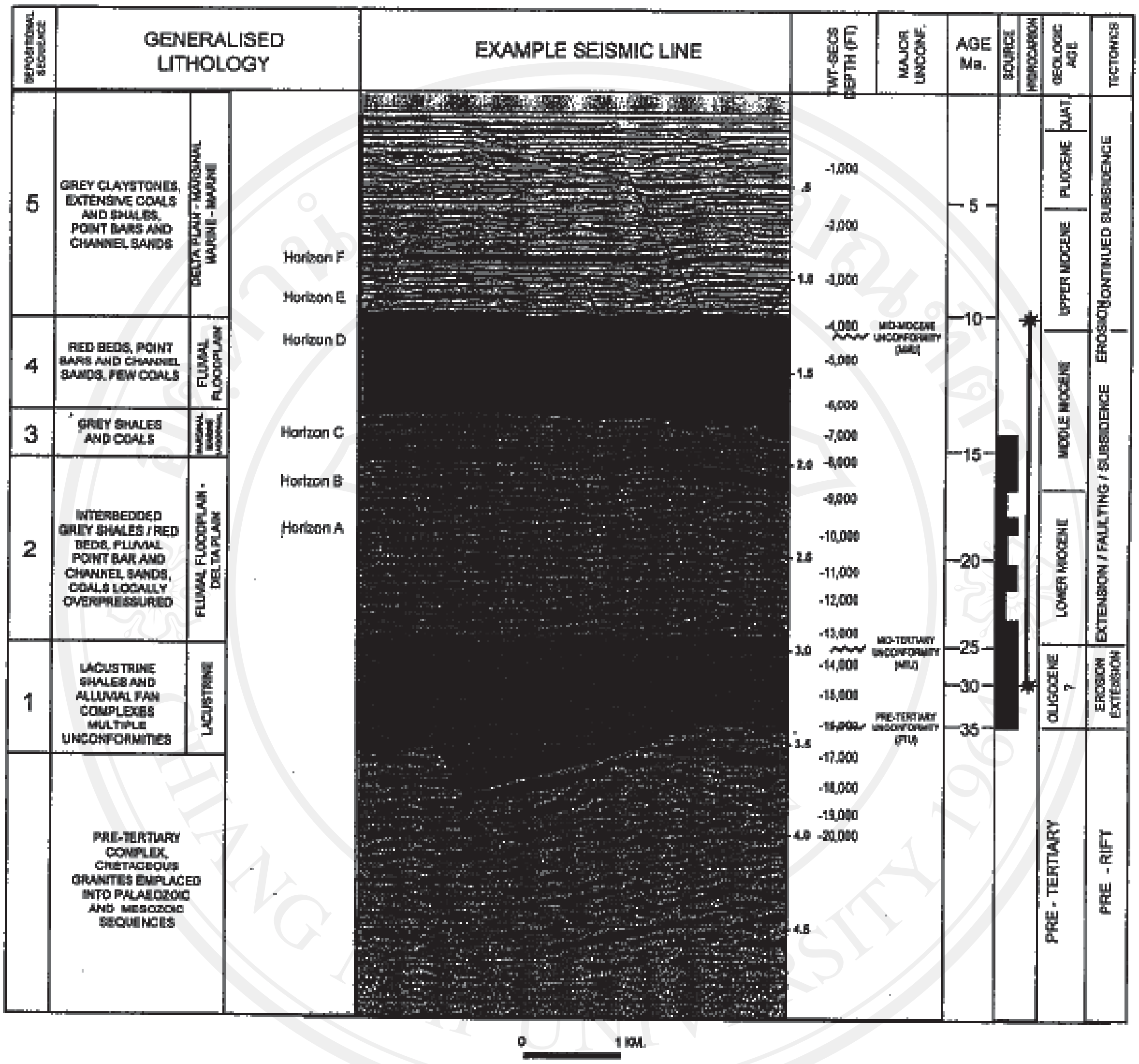

Figure 4.1 Stratigraphic summary in the Pattani Basin is compared six horizons (Modified after Crossley, 1990).

4.2 Structural Development

Development of structural features can be interpreted from change in stratigraphic thickness from footwall to hangingwall of each fault. Figure 4.2 illustrates such changes at fault 3, fault 4, fault 5, fault 6, fault 7 and fault 8. The vertical axis represents the change in stratigraphic thickness from footwall to hangingwall. The change in stratigraphic thickness from footwall to hangingwall of faults is maximum in Unit 1 and decreases with decreasing depth. Increasing gradient of the curve show an increased movement of the fault. Small gradients suggest less movement on faults. As seen in the case of fault 8, the fault is active from Unit 1 to Unit 2, less active from Unit 2 to Unit 3, becomes more active from Units 3 to 4 and decreases in activity onward. Movement on fault 7 constantly decreases from Unit 1 to Unit 5. The activity of faults 3, 4, 5 and 6 decreases sharply from Unit 1 to Unit 2 and gradually decreases from Unit 2 onward. According to these curves, it can be concluded that the faults are more active during the deposition of Unit 1 than Unit 2 to Unit 5. Therefore Unit 1 might be a syn-rift sequence, and the interval of Unit 2 to Unit 5 probably is a post-rift sequence. Packham (1993) suggested that initial rifting was in the Early Oligocene and basin formation was induced by dextral shear. In Middle Miocene, the tectonic activity decreased. Therefore the boundary between syn-rift and post-rift sequences was probably in the Lower Middle Miocene interval. This conforms to the present work. Packham (1993) proposed that local basin inversion and erosion took place during Late Middle Miocene. This erosion was related to the Middle Miocene Unconformity, which can be correlated to 'horizon D' in this work. However, there is no evidence for inversion in the study area. Decrease in tectonism during the Late Miocene to Quaternary concided with the deposition of post-rift sequence. However, the result of this study is dissimilar from Chinbunchorn et al (1989) probably due to the calculation method and local conditions in different basins. The end of rifting in this work is proposed to be early Middle Miocene, which differs from the late Middle Miocene suggested by Chinbunchorn et al. (1989). Deposition of syn-rift sequence corresponded to rifting, extension and rapid subsidence, and, the post-rift phase is characterized by slower subsidence (Chonchawalit, 1993).

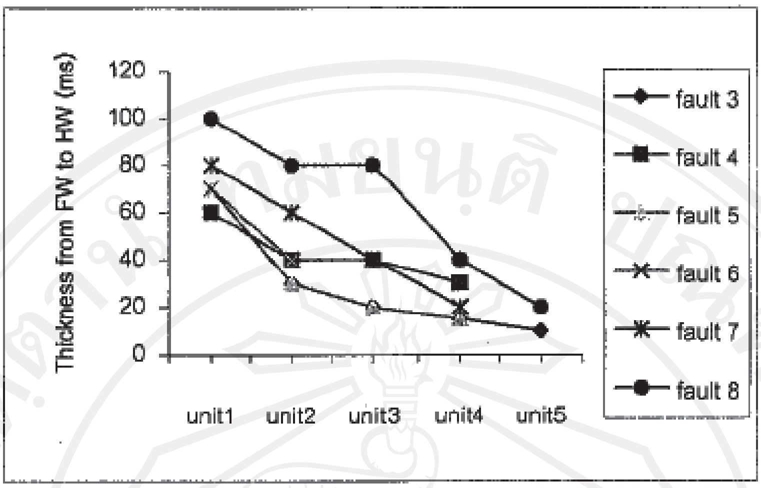

Figure 4.2 Change in stratigraphic thickness of sedimentary units from footwalls to hangingwalls of faults 3, 4, 5, 6, 7 and 8. These changes are determined in unit 1 to unit 5. Fault 8 has maximum changes in stratigraphic thickness and fault 3 has the minimum. The unit of thickness is millisecond.

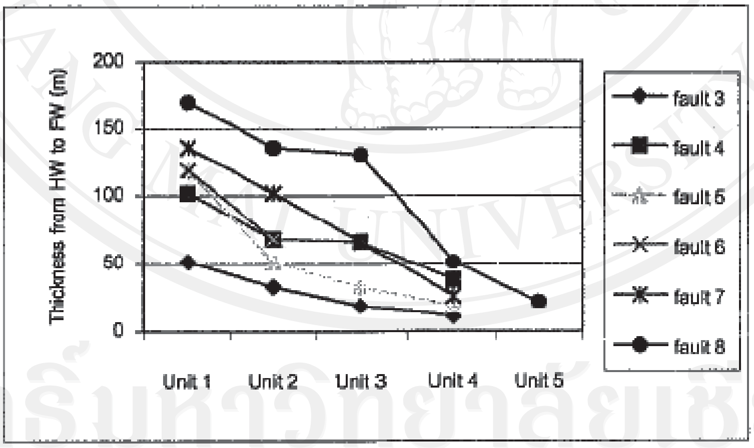

Figure 4.3 Change in stratigraphic thickness of sedimentary units from footwalls to hangingwalls of faults 3, 4, 5, 6, 7 and 8. These changes are determined in unit 1 to unit 5. Fault 8 has maximum changes in stratigraphic thickness and fault 3 has the minimum. The unit of thickness is meters.

4.3 Petroleum Potential

The Pattani basin is the biggest Tertiary rift basin in the Gulf of Thailand and has a petroleum potential (Pradidtan and Dook, 1992). Significant oil and gas reserves have been discovered in the basin. The important characteristics of rift basins that make them exceptional places for petroleum are the sedimentary sequences, rapid subsidence, high geothermal gradient and heat flow (Chinbunchorn et al., 1989). Crossley (1990) suggested that gas and minor quantities of oil in the Pattani Basin have been found in fluvial sandstones.

Oil and gas tend to reach the surface of the Earth and be dissipated. They may encounter a barrier that stops the upward migration and produces a trap. The essential characteristics of a trap are porous and permeable beds, overlain by an impermeable bed that prevents fluid from escaping. The important traps in the Tertiary basins in the Gulf of Thailand are gentle anticline, rollover, tilting fault block and buried hill (Chinbunchorn et al., 1989). In the study area, the structural maps show that the structural closures can be observed in certain footwall and hangingwall areas (Figure 3.12-3.17). These gentle anticlines are intercepted by fault planes. These structural closures include in the footwalls of faults 4 and 5 at horizon A; faults 3, 6 and 7 at horizon B; faults 2, 3, 4 and 7 at horizon C; and faults 1, 2, 3, 4 and 8 at horizon D. Anticline closures also developed in the hangingwall of fault 8 at horizons A and B and the hangingwall of fault 1 at horizon A. The largest closures are in the footwall of faults 7 (Q) and in the hangingwall of fault 8 (W). These traps occur at two horizons making a thick interval with potential for hydrocarbon accumulation. All structural traps are in the Lower Miocene to Middle Miocene sequences. Chinbunchorn et al. (1989) suggested that the Middle Miocene sequence is good seals and is laterally extensive as moderately overpressured section is commonly encountered. According to Pradidtan and Dook (1992), structural closures occur only in the sequences underlying the Late Miocene Unconformity. Numerous oil and gas shows were encountered only in the Lower Miocene sandstones (Lockhart et al., 1997). In the study area there is no structural closure at horizons E and F because less fault slips resulted in less uplift and folding. Potential reservoir sandstones in the

Upper Miocene are insignificant because there is no laterally extensive seal (Chinbunchorn et al., 1989).

To determine petroleum potential, not only appropriate shapes and size of structural traps but also the stratigraphic traps. In the study, although the structural traps are clear on the structural maps but the stratigraphic traps can not be defined because of low resolution. Stratigraphic traps may be interpreted in three dimensional seismic surveys with higher resolution. Stratigraphic traps such as pinched-out sand, distal fan and unconformity are also believed to be important in petroleum exploration in the Pattani Basin (Chinbunchorn et al., 1989).

Seismic horizons in this study were interpreted at regular intervals, to delineate structural development continuously thus the volume of the reservoirs in the traps was not calculated. To calculate the volume of reservoir, the horizon related to petroleum ought to be selected relative to well log data.

4.4 Time-Depth Conversion

Time-depth conversion function in Figure 1.1 was used to find the interval and the average velocities. In Figure 1.1, there are two wells (EH-1 well and Erawan1214 well) which give slightly different velocity functions extracted. In order to construct the structural geometry and evaluate the interpretation, the velocity function should be consistent. However, the two well give somewhat different velocity for each unit, particularly unit 1 and 3. Considering the Erawan 1214 well on the interpreted In-line 107 section (Figure 3.2), it goes through two faults in Unit 1 and 3 which may alter the accuracy of the velocity (Table 4.1). Since EH-1 well passes through a less complicated structure location. Thus its velocity function, table 3.1, was chosen to represent one consistent function for the entire study area.

Horizon	Unit	TWT time (ms)	Depth (m)	Interval Velocity (m/s)	Average Velocity (m/s)	Well Information
	Above 5	0	-	1862		
F		910	847		1862	
	5	220	260	2482		
E		1130	1107		1950	
	4	230	318	2765		
D		1360	1425		2085	
	3	350	540	3086		fault
C		1710	1965		2310	
	2	210	383	3648		
B		1920	2348		2445	
	1	180	277	3078		fault
A		2100	2625		-	

Table 4.1 Data in this table was calculated from Erawan 1214 well data. The TWT times of horizons A to F were picked from the In-line 107 at shotpoint 415 where Erawan 1214 well located. Then the TWT times were converted into depths using time-depth conversion curve of Erawan 1214 well location, Figure 3.11.